RESEARCH ARTICLE

An Electron-Deficient Cp^E Iridium(III) Catalyst: Synthesis, Characterization, and Application to Ether-Directed C–H Amidation

Eiki Tomita,[a] Masahiro Kojima,[a] Yuki Nagashima,[b] Ken Tanaka,[b] Haruki Sugiyama,[c,d] Yasutomo Segawa,[c,d] Atsushi Furukawa,†[a] Katsumi Maenaka,[a,e] Satoshi Maeda,[f,g,h] Tatsuhiko Yoshino,*[a,e] and Shigeki Matsunaga*[a,e]

[a] E. Tomita, Dr. M. Kojima, Dr. A. Furukawa, Prof. Dr. K. Maenaka, Dr. T. Yoshino, Prof. Dr. S. Matsunaga
Faculty of Pharmaceutical Sciences
Hokkaido University
Kita-ku, Sapporo 060-0812, Japan
E-mail: tyoshino@pharm.hokudai.ac.jp; smatsuna@pharm.hokudai.ac.jp
[b] Dr. Y. Nagashima, Prof. Dr. K. Tanaka
Department of Chemical Science and Engineering
Tokyo Institute of Technology
O-okayama, Meguro-ku, Tokyo 152-8550, Japan
[c] Dr. H. Sugiyama, Prof. Dr. Y. Segawa
Institute for Molecular Science
Okazaki 444-8787, Japan
[d] Dr. H. Sugiyama, Prof. Dr. Y. Segawa
Department of Structural Molecular Science
SOKENDAI (The Graduate University for Advanced Studies)
Myodaiji, Okazaki 444-8787, Japan
[e] Prof. Dr. K. Maenaka, Dr. T. Yoshino, Prof. Dr. S. Matsunaga
Global Station for Biosurfaces and Drug Discovery
Hokkaido University
Kita-ku, Sapporo 060-0812, Japan
[f] Prof. Dr. S. Maeda
Institute for Chemical Reaction Design and Discovery (WPI-ICReDD)
Hokkaido University
Kita-ku, Sapporo 001-0021, Japan
[g] Prof. Dr. S. Maeda
Department of Chemistry, Faculty of Science
Hokkaido University
Kita-ku, Sapporo 060-0810, Japan
[h] Prof. Dr. S. Maeda
JST, ERATO Maeda Artificial Intelligence for Chemical Reaction Design and Discovery Project
Kita-ku, Sapporo 060-0810, Japan
[†] Current address
Dr. A. Furukawa
Faculty of Pharmaceutical Sciences, Institute of Medical, Pharmaceutical and Health Sciences
Kanazawa University
Kanazawa 920-1192, Japan

Supporting information for this article is given via a link at the end of the document.

Abstract: The synthesis, characterization, and catalytic performance of an iridium(III) catalyst with an electron-deficient cyclopentadienyl ligand ($[Cp^EIrI_2]_2$) are reported. The $[Cp^EIrI_2]_2$ catalyst was synthesized by complexation of a precursor of the Cp^E ligand with $[Ir(cod)OAc]_2$, followed by oxidation, desilylation, and removal of the COD ligand. The electron-deficient $[Cp^EIrI_2]_2$ catalyst enabled C–H amidation reactions assisted by a weakly coordinating ether directing group. Experimental mechanistic studies and DFT calculations suggested that the high catalytic performance of $[Cp^EIrI_2]_2$ is due to its electron-deficient nature, which accelerates both C–H activation and Ir(V)-nitrenoid formation.

Introduction

Catalytic C–H functionalization reactions, which can directly transform inert C–H bonds into targeted functional groups, are versatile and environmentally benign synthetic methods due to their atom- and step-economy.[1] Group 9 transition-metal complexes with cyclopentadienyl ligands (CpM^{III}; M = Co, Rh, Ir) have been widely used as catalysts for these reactions.[2] The pentamethylcyclopentadienyl (Cp*) ligand is one of the most frequently used ancillary ligands for these complexes because its steric bulkiness and strong electron-donating ability enhance their stability (Scheme 1a).[3] Additionally, appropriate steric and electronic modifications of the Cp ligand can dramatically improve the selectivity and reactivity of the catalysts.[4-10] Steric modifications of Cp ligands generally influence the regio-,[4] diastereo-,[5] site-,[6] chemo-,[7] and enantio-selectivity.[8,9] In contrast, electronic modifications of Cp ligands can influence the reactivity of the catalyst[10] and sometimes change the reaction

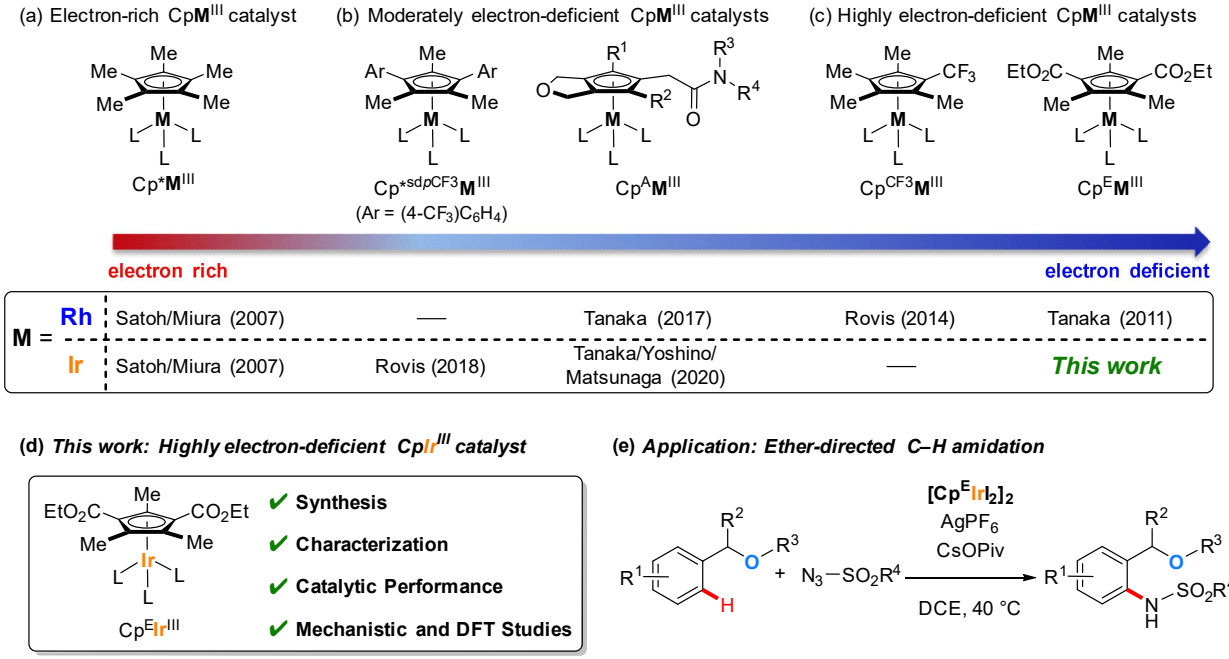

Scheme 1. Modified CpM^{III} catalysts with different electronic properties.

mechanism.[11,12] Electronic tuning by introducing electron-withdrawing groups on the Cp ring to render the metal catalyst electron-deficient and impart unique reactivity has attracted great attention. For example, Rovis and co-workers reported that a CF_3-substituted cyclopentadienyl rhodium (Cp*^{CF3}Rh^{III}) catalyst exhibits higher catalytic activity than a standard Cp*Rh^{III} catalyst in the synthesis of pyridines and dihydropyridines as well as in the cyclopropanation of allylic alcohols (Scheme 1c).[13] One of the authors of this study (K.T.) has developed amide-pendant cyclopentadienyl rhodium (Cp^{A}Rh^{III}) catalysts[11b,d,14] and a bis(ethoxycarbonyl)-substituted cyclopentadienyl rhodium (Cp^{E}Rh^{III}) catalyst (Scheme 1b, c).[11a,c,15] These rhodium catalysts also exhibit high and/or unique reactivity for several C–H functionalization reactions.[14,15]

Despite the success of these electron-deficient modified CpRh^{III} catalysts, limited attention has been paid to the corresponding electron-deficient CpIr^{III} catalysts, which are homologous to the rhodium catalysts but often exhibit complementary catalytic activity.[16] As notable examples, Rovis and co-workers have disclosed that a series of aryl-substituted moderately electron-deficient CpIr^{III} catalysts, such as Cp*^{sdpCF3}Ir^{III}, successfully catalyze the non-directed C–H carbocarbation of anisole derivatives (Scheme 1b).[17,18] In addition, we have developed amide-pendant cyclopentadienyl iridium catalysts (Cp^{A}Ir^{III}) that exhibit high catalytic activity for double aromatic homologation reactions of benzamides by fourfold C–H activation (Scheme 1b).[19] However, the Cp ligands of these catalysts possess only relatively weak electron-withdrawing groups and are thus expected to exhibit merely moderate electron-deficiency. In contrast, the Cp^{E} ligand, which contains two ester groups directly on the cyclopentadienyl ring, should make the corresponding metal catalysts highly electron-deficient.[20] However, this Cp^{E} ligand has only been introduced to rhodium catalysis.[11a,c,15] We speculated that the combination of the Cp^{E} ligand and iridium, which has strong Lewis acidity due to relativistic effects,[21] would afford a novel catalyst with strong Lewis acidity and a highly electrophilic metal center (Cp^{E}Ir^{III}; Scheme 1d). We also envisioned that the Cp^{E}Ir^{III} complex could effectively catalyze weakly directed C–H functionalization reactions,[22] by compensating the weak coordinating ability of the substrates with its high Lewis acidity and electrophilicity.

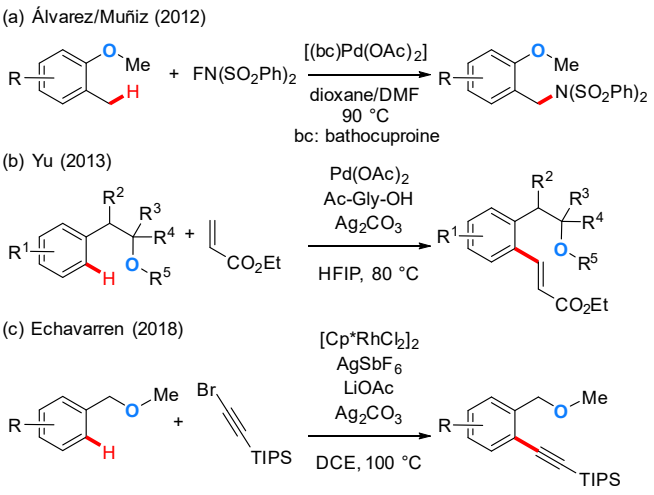

Scheme 2. Examples of ether-directed C–H functionalization reactions catalyzed by high-valent transition-metal catalysts.

Herein, we report the synthesis, characterization, and catalytic performance of a [Cp^{E}IrI$_2$]$_2$ catalyst, which was obtained from the complexation of a precursor of the Cp^{E} ligand with [Ir(cod)OAc]$_2$, followed by oxidation, desilylation, and removal of the COD ligand. We used the [Cp^{E}IrI$_2$]$_2$ complex for ether-directed C–H amidation reactions (Scheme 1e). Compared to nitrogen functional groups or carbonyl groups,[23] the ether group has the

much weaker coordinating ability.[24] Therefore, only limited examples of ether-directed C–H functionalization reactions have been reported, and these methods still suffer from moderate yields, limited substrate scopes, and relatively harsh reaction conditions (Scheme 2).[25-28] The $[Cp^EIrI_2]_2$ catalyst facilitated the benzyl-ether-directed C–H amidation under mild reaction conditions (40 °C in DCE) with a broad substrate scope. We also conducted experimental mechanistic studies and DFT calculations, which revealed that the $[Cp^EIrI_2]_2$ catalyst accelerates both C–H activation and Ir(V)-nitrenoid formation.

Results and Discussion

The $[Cp^ERhCl_2]_2$ complex **2** was previously synthesized by the reductive complexation of fulvene $Cp^{E\text{-}TIPS}$ ligand **1a** with $RhCl_3•nH_2O$ (Scheme 3a).[15] However, the same protocol using $IrCl_3•nH_2O$ failed to afford $[Cp^EIrCl_2]_2$ **3**, and only a complex mixture was obtained (Scheme 3b). Based on our previous report on Cp^AIr complexes,[19] we then tried to synthesize the $[Cp^EIrI_2]_2$ complex via the complexation of $[Ir(cod)OAc]_2$ and the corresponding cyclopentadiene ligand. Although the reduction of **1a** by $NaBH_4$ proceeded smoothly and afforded $Cp^{E\text{-}TIPS}H$ ligand in quantitative yield, the subsequent complexation of $Cp^{E\text{-}TIPS}H$ ligand with $[Ir(cod)OAc]_2$ according to the protocol developed by Cramer and co-workers[29] was unsuccessful, probably due to the steric hindrance of the bulky TIPS group (for details, see Scheme S1). On the other hand, a sterically less hindered $Cp^{E\text{-}TBS}H$ ligand **4**, which was obtained in 95% yield via the reduction of fulvene **1c** using $NaBH_4$, reacted smoothly with $[Ir(cod)OAc]_2$ to give the corresponding iridium complex **5** in 95% yield (Scheme 3c). Oxidation of **5** with two equivalents of I_2 at –78 °C resulted in the formation of COD-coordinated complex **6**.[19,30] Unlike in our previous synthesis of Cp^AIr complexes,[19] the dissociation of the COD ligand and the subsequent dimerization of **6** to directly afford the μ-iodo dimeric complex did not proceed spontaneously in CH_2Cl_2, probably due to the strong coordination of the COD ligand to the highly electron-deficient iridium center. Hence, an alternative synthetic route based on reports by Rheingold and co-workers was investigated;[31] we planned to replace the COD ligand with a CO ligand, which could then be removed via oxidation using NMO. During the investigation of this route, we surprisingly found that the TBS group of **6** was removed under a CO atmosphere to afford desilylated **7** when an appropriate solvent and temperature were selected; it should be noted here that the details of the reaction mechanism of this desilylation process remain unclear at present. After intensive optimization,

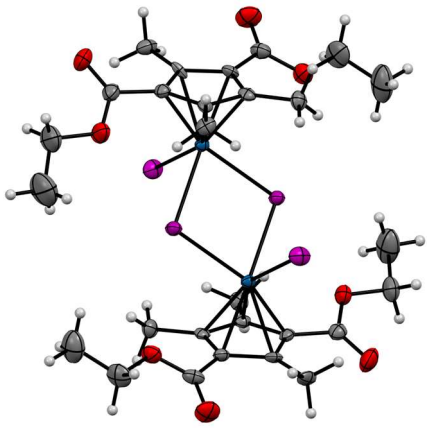

Figure 1. X-ray structure of $[Cp^EIrI_2]_2$ complex **9** with 50% thermal probability.

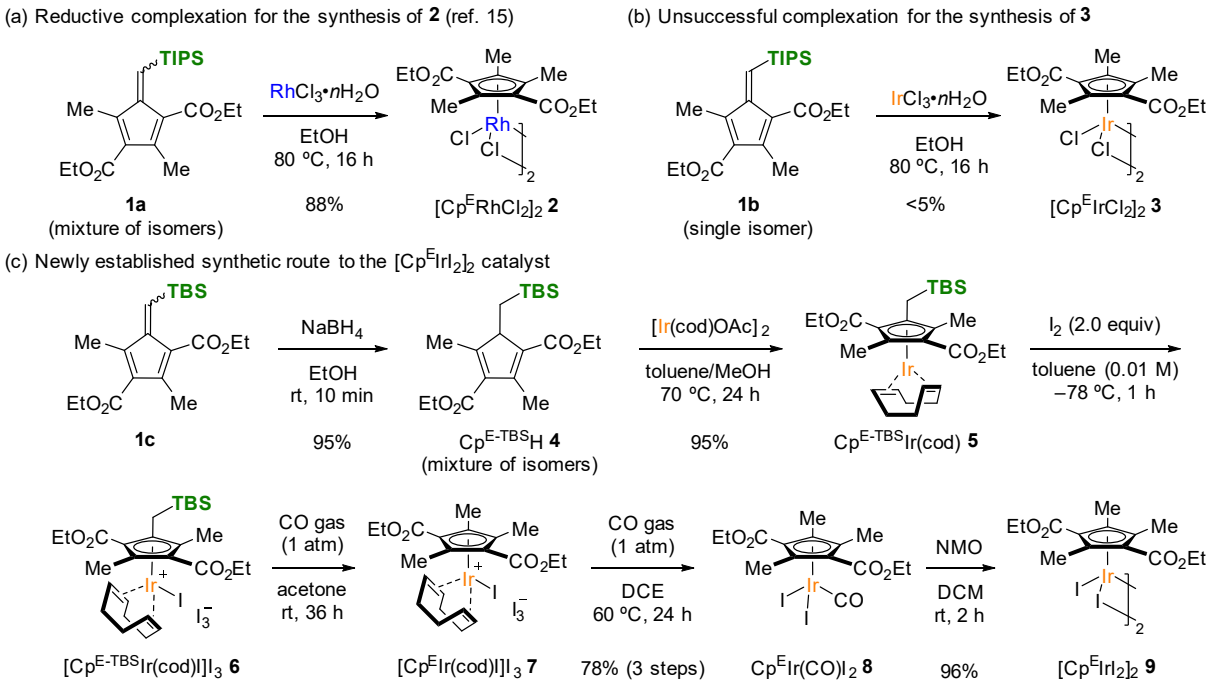

Scheme 3. Synthesis of $[Cp^EIrI_2]_2$ catalyst.

the desilylation reaction was found to proceed effectively under a 1 atm CO atmosphere in acetone at room temperature. The resulting **7** was carbonylated under a 1 atm CO atmosphere in DCE at 60 °C to afford **8**. After purification by silica gel column chromatography, **8** was obtained in 78% yield (3 steps from **5**). Finally, the oxidation of the CO ligand to CO_2 by NMO afforded the desired $[Cp^EIrI_2]_2$ complex **9** in 96% yield. The structure of **9** was unambiguously determined by single crystal X-ray diffraction analysis (Figure 1).[32]

With $[Cp^EIrI_2]_2$ catalyst **9** in hand, we turned our attention to its application in weakly directed C–H functionalization reactions. After several investigations, we found that the C–H amidation reaction of benzyl methyl ether **10a** with TsN_3 **11a** proceeded in almost quantitative yield at 40 °C in DCE when catalytic amounts of **9**, $AgPF_6$, and CsOPiv were used (Table 1, entry 1).[33] As control experiments, we examined the reactivity of other CpM^{III} catalysts under the same conditions (entries 2–9, Figure 2). A standard $[Cp^*IrCl_2]_2$, a moderately electron-deficient $[Cp^{A1}IrI_2]_2$, and $[Cp^{*sdpCF3}IrI_2]_2$ catalyst exhibited inferior reactivity (entries 2–5), highlighting the importance of the highly electron-deficient nature of **9**. Moreover, $[Cp^*RhCl_2]_2$, $[Cp^ERhCl_2]_2$, $[Cp^{A1}RhCl_2]_2$, and $Cp^*Co(CO)I_2$[34] did not give the desired product, and **11a** was recovered quantitatively (entries 6–9). The result with $[Cp^ERhCl_2]_2$ showed that the combination of a Cp^E ligand and iridium is indispensable for this transformation. We also confirmed that the reaction did not proceed in the absence of a catalyst (entry 10).

Table 1. Optimized reaction conditions and control experiments for the ether-directed C–H amidation reaction of **10a** with **11a**.[a]

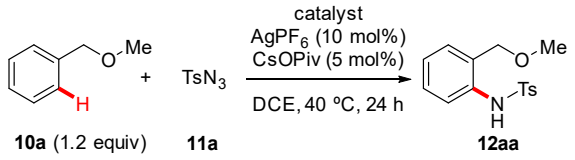

10a (1.2 equiv) **11a** **12aa**

Entry	Catalyst	Yield (%)[b]
1	$[Cp^EIrI_2]_2$ **9** (2.5 mol%)	>95
2	$[Cp^*IrCl_2]_2$ (2.5 mol%)	9
3	$[Cp^{A1}IrI_2]_2$ (2.5 mol%)	<5
4	$[Cp^{*sdpCF3}IrCl_2]_2$ (2.5 mol%)	31
5	$[Cp^{*sdpCF3}IrI_2]_2$ (2.5 mol%)	33
6	$[Cp^ERhCl_2]_2$ (2.5 mol%)	N.R.
7	$[Cp^{A1}RhCl_2]_2$ (2.5 mol%)	N.R.
8	$[Cp^*RhCl_2]_2$ (2.5 mol%)	N.R.
9	$Cp^*Co(CO)I_2$ (5 mol%)	N.R.
10	none	N.R.

[a] Reaction conditions: **10a** (0.060 mmol), **11a** (0.050 mmol), catalyst (0.00125 mmol), $AgPF_6$ (0.0050 mmol), and CsOPiv (0.0025 mmol) in DCE (0.50 mL) at 40 °C for 24 h under an argon atmosphere. [b] The yields were determined via ^1H NMR analysis of the crude mixture using 1,1,2,2-tetrachloroethane as an internal standard.

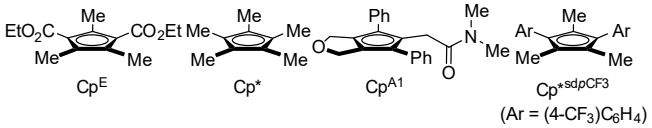

Figure 2. Structures of Cp ligands applied for this study.

The substrate scope and limitations of the ether-directed C–H amidation reactions are summarized in Scheme 4. Model substrate **10a** gave **12aa** in 91% isolated yield. Substituents at the *para* position were well tolerated; alkyl- (**12ba**–**12da**), phenyl- (**12ea**), halogen- (**12fa**–**11ia**), Bpin- (**12ja**), and OCF_3-substituted (**12ka**) ethers afforded the corresponding amidated products in moderate to good yield, and *meta*-halogen-substituted ethers were also compatible (**12la**–**12na**). We also investigated substrates bearing various *ortho*-substituents, including halogen (**12oa**–**12ra**), methyl (**12sa**), and CF_3 (**12ta**) groups, which afforded the products in 50–91% yields. In addition, a methyl substituent at the benzylic position was tolerated in this reaction, and **12ua** was obtained in 77% yield. Furthermore, six- and five-membered cyclic ethers also successfully acted as directing groups, furnishing the corresponding products in 99% (**12va**) and 63% yield (**12wa**). With ethyl and *n*-butyl ethers, the reactivity was somewhat decreased as the steric hindrance increased (**12xa**, **12ya**). Ethers with additional coordinating functional groups were also investigated (**12za**–**12aca**). When an ester-substituted ether was used, the C–H amidation reactions directed by the ether and by the ester competed without selectivity, but doubly amidated **12za** was obtained in 71% yield in the presence of 2.5 equivalents of **11a**. On the other hand, a ketone-substituted ether was amidated selectively at the *ortho*-position to the ketone moiety, affording**12aaa** in 97% yield. Substrates containing a pyridine ring and a cyano group were not applicable with this reaction probably due to the strong coordination of these groups to the Ir metal center (**12aba**, **12aca**). Other unsuccessful substrates were summarized in Figure S1.

The scope of sulfonyl azides **11** was subsequently investigated (Scheme 4, bottom). Phenyl sulfonyl azide and 1-naphthyl sulfonyl azide furnished the expected products in good yields (**12ab**, **12ag**). Aryl sulfonyl azides with electron-donating or -withdrawing substituents reacted smoothly to give the corresponding amidated products in moderate to good yields (**12ac**–**12af**). Alkyl sulfonyl azides were also applicable without difficulty (**12ah**, **12ai**). In addition, sulfonyl azide with bulky mesityl group aforrded **12aj** in 67% yield. Notably, the difunctionalization of *ortho*-C–H bonds, which was problematic in previously reported ether-directed C–H functionalization reactions,[26,27] was not observed for any of the investigated substrates in Scheme 4. Other amidating/aminating reagents, such as dioxazolone, aryl- or alkylazides, did not furnish the desired products under the current reaction conditions (for details, see Figure S1).

To confirm the scalability of this reaction, a gram-scale reaction was conducted using model substrate **10a**, which

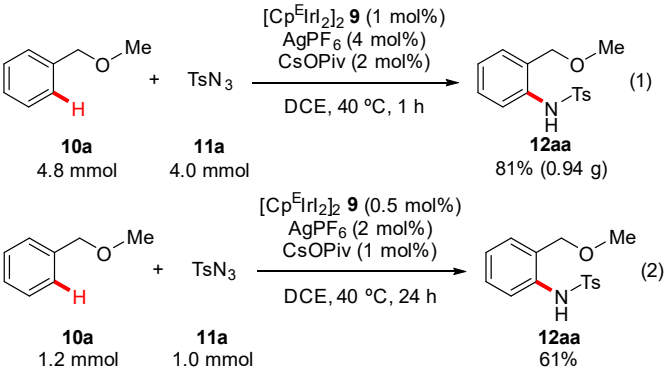

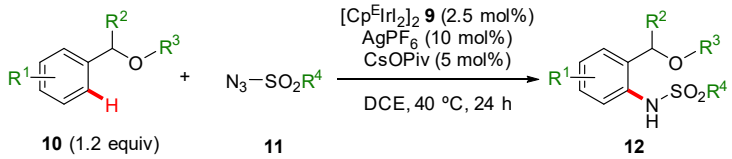

Scope of ethers[a]

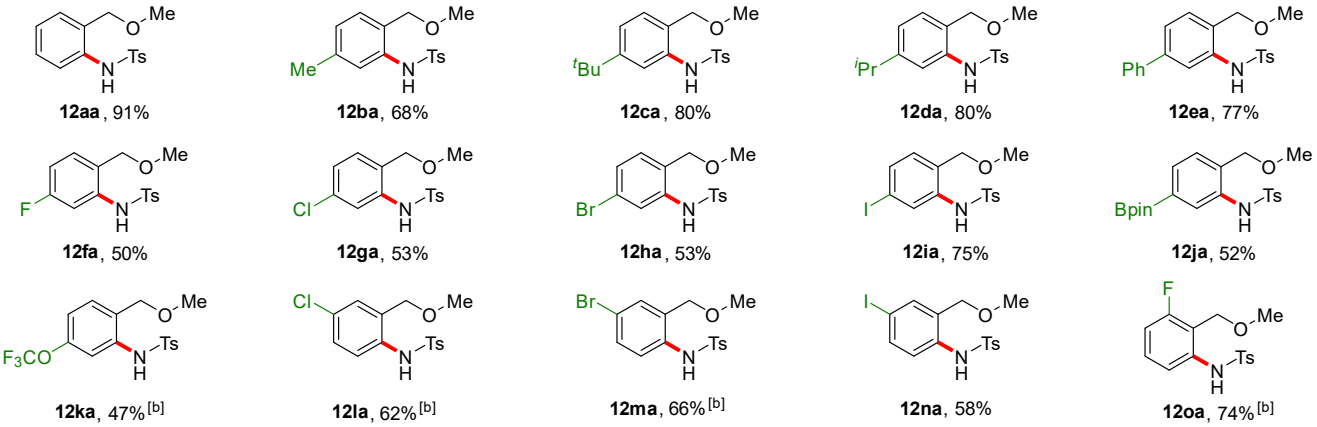

Scope of sulfonyl azides[a]

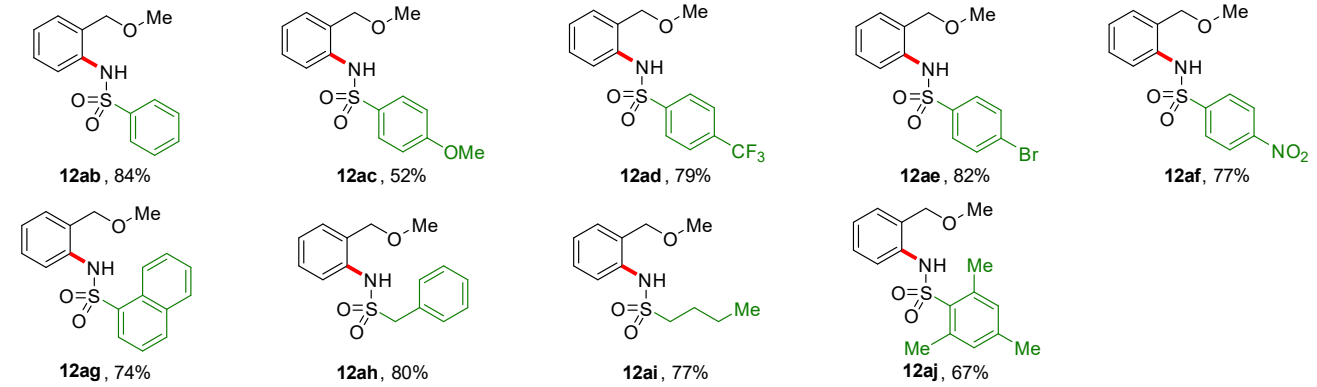

Scheme 4. Substrate scope and limitations of the ether-directed C–H amidation reaction between **10** and **11**. [a] Reaction conditions: **10** (0.24 mmol), **11** (0.20 mmol), **9** (0.0050 mmol), $AgPF_6$ (0.020 mmol) and CsOPiv (0.010 mmol) in DCE (2 mL) at 40 °C for 24 h. [b] **9** (0.010 mmol, 5 mol%), $AgPF_6$ (0.040 mmol, 20 mol%), and CsOPiv (0.020 mmol, 10 mol%). [c] **10z** (0.20 mmol), **11a** (0.50 mmol, 2.5 equiv), **9** (0.010 mmol, 5 mol%), $AgPF_6$ (0.040 mmol, 20 mol%) and CsOPiv (0.020 mmol, 10 mol%).

furnished **12aa** in 81% yield (0.94 g) with a low catalyst loading of **9** (1 mol%) in a short reaction time (1 h; eq 1). When the catalyst loading was further reduced to 0.5 mol%, **12aa** was obtained in 61% yield (eq 2).

The distinctive reactivity of **9** in the ether-directed C–H amidation prompted us to clarify the difference among **9**, Cp*^{sdpCF3}Ir, and Cp*Ir complexes. To evaluate the electronic nature of the Ir center of the catalyst, we synthesized triethylphosphite-coordinated complexes Cp^{E}Ir(P(OEt)$_3$)I$_2$ **13**, Cp*^{sdpCF3}Ir(P(OEt)$_3$)I$_2$ **14**, and Cp*Ir(P(OEt)$_3$)I$_2$ **15** (for details, see the Supporting Information), which we used in Gutmann–Beckett-type experiments.[35] The chemical shift of the ^{31}P NMR signal of **13** exhibited a large upfield shift relative to that of **15** (70.18 ppm to 56.50 ppm; Figure 3a), which demonstrates the higher electron-deficiency of **13** compared to that of **15**. The ^{31}P NMR signal of **14** (57.32 ppm) was between those of **13** and **15,** albeit closer to that of **13**. This behavior is similar to that observed in previous studies of modified CpRh complexes.[10b,20] We also measured the CO stretching frequencies of the complexes Cp^{E}Ir(CO)I$_2$ **8**, Cp*^{sdpCF3}Ir(CO)I$_2$ **16**, and Cp*Ir(CO)I$_2$ **17** using IR spectroscopy (Figure 3b).[10b,20] Much higher CO stretching frequencies were observed for **8** (2050.9 cm^{-1}) and **16** (2050.9 cm^{-1}) compared to that of **17** (2016.2 cm^{-1}). These values reflect the weaker π-back donation in the Cp^{E}Ir and Cp*^{sdpCF3}Ir complexes compared to that in the Cp*Ir complex, which supports the electron-deficient nature of these complexes. The cyclic voltammogram of [Cp*IrI$_2$]$_2$ **19** exhibited an irreversible anodic peak current at +0.15 V vs. Fc/Fc$^+$, which probably corresponds to the oxidation of Ir^{III} to Ir^{IV} (Figure 3c). The cyclic voltammogram of **9** also showed an irreversible oxidation, albeit at a much higher potential (+0.81 V vs. Fc/Fc$^+$), while that of [Cp*^{sdpCF3}IrI$_2$]$_2$ **18** showed an intermediate oxidation potential (+0.70 V vs. Fc/Fc$^+$). The higher oxidation potential of **9** compared to those of **18** and **19** was also attributed to its highly electron-deficient nature. All these experimental observations

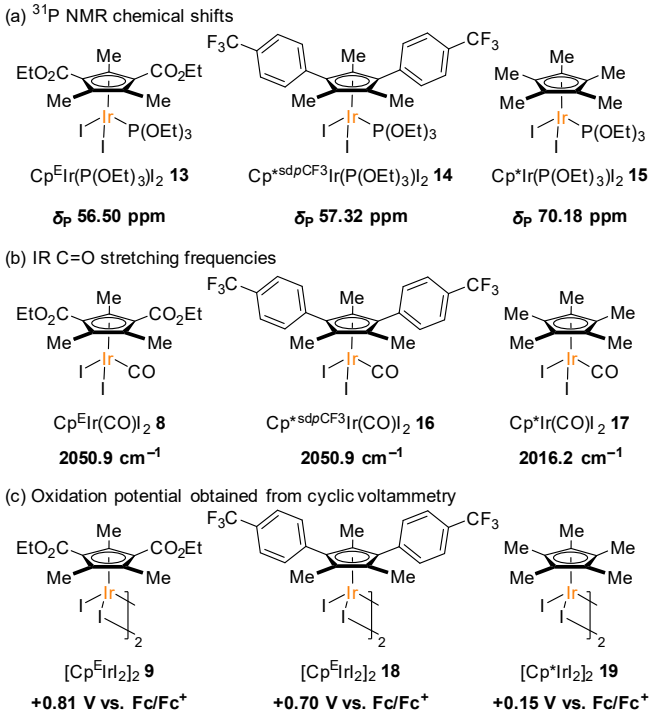

Figure 3. Evaluation of the electronic nature of the Ir center.

supported the highly electron-deficient nature of **9**.

To shed light on the mechanistic aspects of the present ether-directed C–H amidation reaction, kinetic isotope effect (KIE) experiments were performed. In parallel experiments using undeuterated **10a** and deuterated **10a**-d_4, a primary KIE was observed (k_H/k_D = 3.17; eq 3), which implied that C–H bond cleavage may be involved in the rate-determining step.[36]

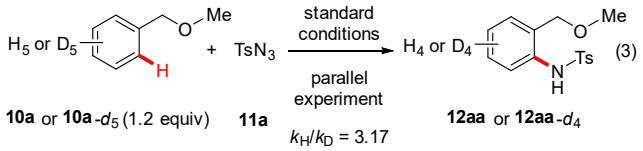

We also performed kinetic studies to reveal the dependence of the reaction rate on the concentrations of ether **10a**, azide **11a**, and the catalyst (for details, see the Supporting Information). While a near first-order dependence (1.19) was observed for the catalyst, Michaelis–Menten type saturation kinetics were observed for **10a** and **11a**.[37] These results indicated that both C–H activation and Ir(V)-nitrenoid formation would be similarly slow, and both steps could be rate-determining depending on the reaction conditions. In addition, the product inhibition was not observed for this reaction.

We conducted DFT calculations of the mechanism of the ether-directed C–H amidation reaction to gain further insight into the reason for the high reactivity of **9**. A full catalytic cycle was calculated at the B3LYP-D3/6-311++G**, SDD =Ir, CPCM(DCE)//B3LYP-D3/6-31G**, LanL2DZ=Ir, CPCM(DCE) level of theory for a highly electron-deficient Cp^{E}Ir catalyst as well as for a moderately electron-deficient Cp*^{sdpCF3}Ir catalyst and an electron-rich Cp*Ir catalysts for comparison. The plausible catalytic cycle for these catalysts and the activation energies of each step are summarized in Figure 4 (for full energy diagrams, see Scheme S2). The catalytic cycle begins with the generation of the active cationic complex from [Cp^{x}IrX$_2$]$_2$ (X = Cl or I), AgPF$_6$, and CsOPiv. The subsequent C–H activation occurs via a pivalate-assisted concerted-metalation deprotonation (CMD) mechanism,[38] and the activation barrier for this step is 17.7 kcal/mol for Cp^{E}Ir, 17.6 kcal/mol for Cp*^{sdpCF3}Ir, and 21.4 kcal/mol for Cp*Ir. Although there is no clear energy difference between Cp^{E}Ir and Cp*^{sdpCF3}Ir for this step, a high activation energy is required with the Cp*Ir catalyst, suggesting that the electron-deficient catalysts facilitate the C–H activation. After the C–H activation, ligand exchange with TsN$_3$, followed by N$_2$ extrusion gives an Ir(V)-nitrenoid intermediate.[39] The overall activation energy for the Ir(V)-nitrenoid formation is significantly lower with Cp^{E}Ir (18.4 kcal/mol) than with Cp*^{sdpCF3}Ir (20.7 kcal/mol) or Cp*Ir (22.5 kcal/mol). The subsequent C–N bond formation exhibits similar barriers regardless of the ligands, and the final protodemetalation step is an almost-barrierless process. In the case of the Cp^{E}Ir-catalyzed reaction, the difference between the activation energies for the C–H activation (17.6 kcal/mol) and the formation of the Ir(V)-nitrenoid (18.3 kcal/mol) is small (<1 kcal/mol). The calculated energy profile, as well as the experimental mechanistic studies, suggest that both C–H activation and the formation of the Ir(V)-nitrenoid are kinetically relevant. The results of several additional computational studies suggest that the electron-deficient Cp^{E} ligand can strengthen the interaction between the ether substrate and metal catalyst, which

leads to stabilization of the transition state for the C–H activation as well as the metallacycle intermediate.[40] The stabilization of the metallacycle intermediate would then eventually lower the activation energy for the subsequent Ir(V)-nitrenoid formation (for details, see the Supporting Information).

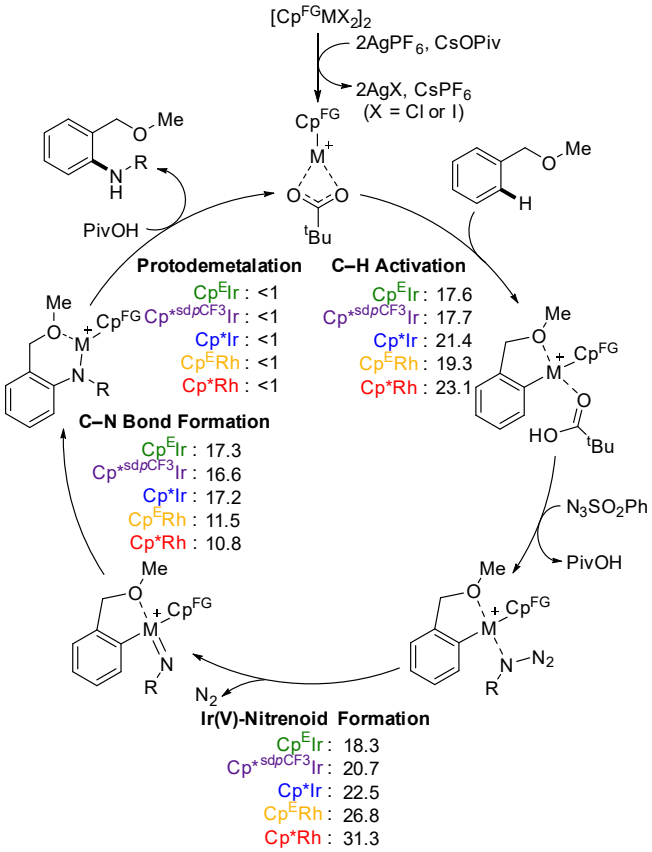

Figure 4. Plausible catalytic cycle and calculated activation energies $\Delta G^{\ddagger}$ (kca/mol). Gibbs free energies were obtained at the B3LYP-D3/6-311++G**, SDD=Ir, CPCM(DCE)//B3LYP-D3/6-31G**, LanL2DZ=Ir, CPCM(DCE) level of theory.

The full catalytic cycle with Cp*Rh or Cp^{E}Rh catalysts was also calculated at the same level (for details, see Scheme S3). The activation barriers for the cleavage of the C–H bond (Cp^{E}Rh: 19.3 kcal/mol; Cp*Rh: 23.1 kcal/mol) are slightly higher than those with the Ir catalysts, albeit still feasible. In contrast, the activation energies required for the formation of the Rh(V)-nitrenoid are considerably higher than those for the formation of the Ir(V)-nitrenoid (Cp^{E}Rh: 26.8 kcal/mol; Cp*Rh: 31.3 kcal/mol). The Rh(V)-nitrenoid formation is by ca. 15 kcal/mol less exergonic than the Ir(V)-nitrenoid formation. The higher activation barrier and lower exergonicity for the Rh(V)-nitrenoid formation can be attributed to the weaker Rh=N bond compared to the Ir=N bond.[21c,d,41] The subsequent insertion and protonation steps exhibit reasonably low activation barriers. Overall, the Rh catalysts are unsuitable for the present reaction due to the difficulty of Rh(V)-nitrenoid formation, and thus, the use of the electron-deficient Cp^{E}Ir catalyst is crucial to the successful ether-directed C–H amidation reaction under mild conditions.

Conclusion

In conclusion, we have synthesized and characterized an iridium(III) catalyst with a highly electron-deficient cyclopentadienyl ligand ([Cp^{E}IrI$_2$]$_2$), which catalyzes ether-directed C–H amidation reactions under mild reaction conditions. The catalytic activity of other related group 9 metal catalysts, such as the Cp*Ir, Cp*Rh, and Cp^{E}Rh catalysts, is greatly inferior to that of Cp^{E}Ir. Experimental and computational mechanistic studies revealed that the high reactivity of the Cp^{E}Ir complex is due to its high electron-deficiency, which accelerate both the activation of the C–H bond and the formation of the Ir(V)-nitrenoid, while the corresponding Cp^{E}Rh catalyst is not suitable for the formation of the nitrenoid species under such mild conditions. Our results demonstrate the importance of the combination of the highly electron-deficient Cp^E ligand with an iridium center to achieve high reactivity in challenging ether-directed C–H amidation reactions. Based on its distinct properties, the Cp^{E}Ir catalyst may find further applications in C–H functionalization reactions and other synthetic organic transformations in which other related metal catalysts show insufficient reactivity.

Acknowledgements

This work was supported in part by JSPS KAKENHI Grant Number JP20H02730 (S.M.), JP20H04794 in Hybrid Catalysis (T.Y.), JP21K05046 (T.Y.), JP21K14623 (Y.N.), JP22H05346 (Y.N.) and JP22H05327 (T.Y.) in Transformative Research Areas (A) JP21A204 Digitalization-driven Transformative Organic Synthesis (Digi-TOS), and JSPS Fellowship JP21J21168 (E.T.). This work was in part supported by JSPS World Premier International Research Center Initiative (WPI). One of the authors (E.T.) was supported by Hokkaido University through the Program for Leading Graduate Schools (Hokkaido University "Ambitious Leader's Program"). This work was also partly supported by Hokkaido University, Global Facility Center (GFC), Pharma Science Open Unit (PSOU), funded by MEXT under the "Support Program for Implementation of New Equipment Sharing System".

Keywords: iridium • Cp^E ligand • C–H activation • ether directing group • amidation

[1] a) B. M. Trost, *Science* **1991**, *254*, 1471–1477; b) P. A. Wender, B. L. Miller, *Nature* **2009**, *460*, 197–201.

[2] a) K. Ueura, T. Satoh, M. Miura, *Org. Lett.* **2007**, *9*, 1407–1409; b) T. Satoh, M. Miura, *Chem. Eur. J.* **2010**, *16*, 11212–11222; c) N. Kuhl, N. Schröder, F. Glorius, *Adv. Synth. Catal.* **2014**, *356*, 1443–1460; d) G. Song, X. Li, *Acc. Chem. Res.* **2015**, *48*, 1007–1020; e) K. Shin, H. Kim, S. Chang, *Acc. Chem. Res.* **2015**, *48*, 1040–1052; f) T. Yoshino, S. Matsunaga, *Adv. Synth. Catal.* **2017**, *359*, 1245–1262; g) X. Li, W. Ouyang, J. Nie, S. Ji, Q. Chen, Y. Huo, *ChemCatChem* **2020**, *12*, 2358–2384.

[3] J. F. Hartwig, *Organotransition Metal Chemistry: From Bonding to Catalysis*, University Science Books, Sausalito, CA, **2010**.

[4] For selected examples of regioselective C–H functionalization reactions catalyzed by modified CpRh^{III} catalysts, see: a) T. K. Hyster, T. Rovis, *Chem. Sci.* **2011**, *2*, 1606–1610; b) T. K. Hyster, T. Rovis, *Chem. Commun.* **2011**, *47*, 11846–11848; c) M. D. Wodrich, B. Ye, J. F. Gonthier, C. Corminboeuf, N. Cramer, *Chem. Eur. J.* **2014**, *20*, 15409–15418; d) T. K. Hyster, D. M. Dalton, T. Rovis, *Chem. Sci.* **2015**, *6*, 254–258; e) B. Li, J. Yang, H. Xu, H. Song, B. Wang, *J. Org. Chem.* **2015**, *80*, 12397–12409; f) E. A. Trifonova, N. M. Ankudinov, M. V. Kozlov, M. Y. Sharipov, Y. V. Nelyubina, D. S. Perekalin, *Chem. Eur. J.* **2018**, *24*, 16570–16575; g) J. Terasawa, Y. Shibata, Y. Kimura, K. Tanka, *Chem.*

Asian J. **2018**, *13*, 505–509; h) J. S. Barber, S. Scales, M. Tran-Dubé, F. Wang, N. W. Sach, L. Bernier, M. R. Collins, J. Zhu, I. J. McAlpine, R. L. Patman, *Org. Lett.* **2019**, *21*, 5689–5693; i) S. Lee, N. Semakul, T. Rovis, *Angew. Chem. Int. Ed.* **2020**, *59*, 4965–4969; *Angew. Chem.* **2020**, *132*, 4995–4999.

[5] For selected examples of diastereoselective C–H functionalization reactions catalyzed by modified $CpRh^{III}$ catalysts, see: a) T. Piou, T. Rovis, *J. Am. Chem. Soc.* **2014**, *136*, 11292–11295; b) N. Semakul, K. E. Jackson, R. S. Paton, T. Rovis, *Chem. Sci.* **2017**, *8*, 1015–1020; c) T. Piou, F. Romanov-Michailidis, M. A. Ashley, M. Romanova-Michaelides, T. Rovis, *J. Am. Chem. Soc.* **2018**, *140*, 9587–9593; d) F. Burg, T. Rovis, *J. Am. Chem. Soc.* **2021**, *143*, 17964–17969; e) F. Burg, T. Rovis, *ACS Catal.* **2022**, *12*, 9690–9697.

[6] H. Lei, T. Rovis, *Nat. Chem.* **2020**, *12*, 725–731.

[7] a) T. Piou, T. Rovis, *Nature* **2015**, *527*, 86–90; b) L. Li, H. Gao, M. Sun, Z. Zhou, W. Yi, *Org. Lett.* **2020**, *22*, 5473–5478.

[8] For selected examples of enantioselective C–H functionalization reactions catalyzed by chiral CpM^{III} catalysts, see: a) T. K. Hyster, L. Knörr, T. R. Ward, T. Rovis, *Science* **2012**, *338*, 500–503; b) B. Ye, N. Cramer, *Science* **2012**, *338*, 504–506; c) B. Ye, N. Cramer, *J. Am. Chem. Soc.* **2013**, *135*, 636–639; d) M. Dieckmann, Y.-S. Jang, N. Cramer, *Angew. Chem. Int. Ed.* **2015**, *54*, 12149–12152; *Angew. Chem.* **2015**, *127*, 12317–12320; e) J. Zheng, W.-J. Cui, C. Zheng, S.-L. You, *J. Am. Chem. Soc.* **2016**, *138*, 5242–5245; f) Z.-J. Jia, C. Merten, R. Gontla, C. G. Daniliuc, A. P. Antonchick, H. Waldmann, *Angew. Chem. Int. Ed.* **2017**, *56*, 2429–2434; *Angew. Chem.* **2017**, *129*, 2469–2474; g) E. A. Trifonova, N. M. Ankudinov, A. A. Mikhaylov, D. A. Chusov, Y. V. Nelyubina, D. S. Perekalin, *Angew. Chem. Int. Ed.* **2018**, *57*, 7714–7718; *Angew. Chem.* **2018**, *130*, 7840–7844; h) K. Ozols; Y.-S. Jang, N. Cramer, *J. Am. Chem. Soc.* **2019**, *141*, 5675–5680; i) G. Li, X. Yan, J. Jiang, H. Liang, C. Zhou, J. Wang, *Angew. Chem. Int. Ed.* **2020**, *59*, 22436–22440; *Angew. Chem.* **2020**, *132*, 22622–22626; j) C. M. B. Farr, A. M. Kazerouni, B. Park, C. D. Poff, J. Won, K. R. Sharp, M.-H. Baik, S. B. Blakey, *J. Am. Chem. Soc.* **2020**, *142*, 13996–14004; k) J. Mas-Roselló, A. G. Herraiz, B. Audic, A. Laverny, N. Cramer, *Angew. Chem. Int. Ed.* **2021**, *60*, 13198–13224; *Angew. Chem.* **2021**, *133*, 13306–13332; l) X. Yan, J. Jiang, J. Wang, *Angew. Chem. Int. Ed.* **2022**, *61*, e202201522; *Angew. Chem.* **2022**, *134*, e202201522; m) X. Yan, J. Wang, *Synthesis* **2023**, DOI: 10.1055/a-2005-5006

[9] For selected examples of enantioselective C–H functionalization reactions catalyzed by achiral modified CpM^{III} catalysts with chiral carboxylic acids, see: a) L. Lin, S. Fukagawa, D. Sekine, E. Tomita, T. Yoshino, S. Matsunaga, *Angew. Chem. Int. Ed.* **2018**, *57*, 12048–12052; *Angew. Chem.* **2018**, *130*, 12224–12228; b) S. Fukagawa, Y. Kato, R. Tanaka, M. Kojima, T. Yoshino, S. Matsunaga, *Angew. Chem. Int. Ed.* **2019**, *58*, 1153–1157; *Angew. Chem.* **2019**, *131*, 1165–1169; c) W. Liu, W. Yang, J. Zhu, Y. Guo, N. Wang, J. Ke, P. Yu, C. He, *ACS Catal.* **2020**, *10*, 7207–7215; d) T. Yoshino, S. Matsunaga, *ACS Catal.* **2021**, *11*, 6455–6466.

[10] a) T. A. Davis, C. Wang, T. Rovis, *Synlett* **2015**, *26*, 1520–1524; b) W. Lin, W. Li, D. Lu, F. Su, T.-B. Wen, H.-J. Zhang, *ACS Catal.* **2018**, *8*, 8070–8076; c) R. Yoshimura, K. Tanaka, *Chem. Eur. J.* **2020**, *26*, 4969–4973; d) J. Tanaka, Y. Nagashima, K. Tanaka, *Org. Lett.* **2020**, *22*, 7181–7186; e) V. B. Kharitonov, D. V. Muratov, Y. V. Nelyubina, D. A. Loginov, *Synthesis* **2022**, *54*, 5119–5127; f) N. Wagner-Carlberg, T. Rovis, *J. Am. Chem. Soc.* **2022**, *144*, 22426–22432; g) M. Peng, C.-S. Wang, P.-P. Chen, T. Roisnel, H. Doucet, K. N. Houk, J.-F. Soulé, *J. Am. Chem. Soc.* **2023**, *145*, 4508–4516.

[11] a) S. Y. Hong, J. Jeong, S. Chang, *Angew. Chem. Int. Ed.* **2017**, *56*, 2408–2412; *Angew. Chem.* **2017**, *129*, 2448–2452; b) T. Yamada, Y. Shibata, S. Kawauchi, S. Yoshizaki, K. Tanaka, *Chem. Eur. J.* **2018**, *24*, 5723–5727; c) Y. Honjo, Y. Shibata, K. Tanaka, *Chem. Eur. J.* **2019**, *25*, 9427–9432; d) T. Yamada, Y. Shibata, K. Tanaka, *Chem. Eur. J.* **2019**, *25*, 16022–16031.

[12] For a review on the modified $CpRh^{III}$ complexes, see: T. Piou, T. Rovis, *Acc. Chem. Res.* **2018**, *51*, 170–180.

[13] a) J. M. Neely, T. Rovis, *J. Am. Chem. Soc.* **2014**, *136*, 2735–2738; b) F. Romanov-Michailidis, K. F. Sedillo, J. M. Neely, T. Rovis, *J. Am. Chem. Soc.* **2015**, *137*, 8892–8895; c) E. J. T. Phipps, T. Rovis, *J. Am. Chem. Soc.* **2019**, *141*, 6807–6811; d) E. J. T. Phipps, T. Piou, T. Rovis, *Synlett* **2019**, *30*, 1787–1790.

[14] a) S. Yoshizaki, Y. Shibata, K. Tanaka, *Angew. Chem. Int. Ed.* **2017**, *56*, 3590–3593; *Angew. Chem.* **2017**, *129*, 3644–3647; b) T. Yamada, Y. Shibata, K. Tanaka, *Asian J. Org. Chem.* **2018**, *7*, 1396–1402; c) R. Yoshimura, Y. Shibata, T. Yamada, K. Tanaka, *J. Org. Chem.* **2019**, *84*, 2501–2511; d) R. Yoshimura, Y. Shibata, S. Yoshizaki, J. Terasawa, T. Yamada, K. Tanaka, *Asian J. Org. Chem.* **2019**, *8*, 986–993; e) J. Tanaka, Y. Shibata, A. Joseph, J. Nogami, J. Terasawa, R. Yoshimura, K. Tanaka, *Chem. Eur. J.* **2020**, *26*, 5774–5779; f) J. Tanaka, Y. Nagashima, A. J. Araujo Dias, K. Tanaka, *J. Am. Chem. Soc.* **2021**, *143*, 11325–11331.

[15] a) Y. Shibata, K. Tanaka, *Angew. Chem. Int. Ed.* **2011**, *50*, 10917–10921; *Angew. Chem.* **2011**, *123*, 11109–11113; b) K. Morimoto, M. Itoh, K. Hirano, T. Satoh, Y. Shibata, K. Tanaka, M. Miura, *Angew. Chem. Int. Ed.* **2012**, *51*, 5359–5362; *Angew. Chem.* **2012**, *124*, 5455–5458; c) Y. Hoshino, Y. Shibata, K. Tanaka, *Adv. Synth. Catal.* **2014**, *356*, 1577–1585; d) M. Fukui, Y. Hoshino, T. Satoh, M. Miura, K. Tanaka, *Adv. Synth. Catal.* **2014**, *356*, 1638–1644; e) Y. Honjo, Y. Shibata, E. Kudo, T. Namba, K. Masutomi, K. Tanaka, *Chem. Eur. J.* **2018**, *24*, 317–321; f) M. Font, B. Cendón, A. Seoane, J. L. Mascareñas, M. Gulías, *Angew. Chem. Int. Ed.* **2018**, *57*, 8255–8259; *Angew. Chem.* **2018**, *130*, 8387–8391; g) R. Yoshimura, Y. Shibata, K. Tanaka, *J. Org. Chem.* **2019**, *84*, 13164–13171; h) G. Mihara, K. Ghosh, Y. Nishii, M. Miura, *Org. Lett.* **2020**, *22*, 5706–5711; i) H. Takahashi, Y. Honjo, Y. Shibata, Y. Nagashima, K. Tanaka, *Synthesis* **2021**, *53*, 3065–3074; j) Y. Nagashima, S. Ishigaki, J. Tanaka, K. Tanaka, *ACS Catal.* **2021**, *11*, 13591–13602; k) H. Gao, L. Hu, Y. Hu, X. Lv, Y.-B. Wu, G. Lu, *Org. Chem. Front.* **2022**, *9*, 979–988.

[16] a) K. Ueura, T. Satoh, M. Miura, *J. Org. Chem.* **2007**, *72*, 5362–5367; b) J. Park, S. Chang, *Chem. Asian J.* **2018**, *13*, 1089–1102; c) S. Yamane, T. Hinoue, Y. Usuki, M. Itazaki, H. Nakazawa, Y. Hayashi, S. Kawauchi, M. Miura, T. Satoh, *Chem. Eur. J.* **2018**, *24*, 7852–7855; d) Q.-L. Yang, Y.-K. Xing, X.-Y. Wang, H.-X. Ma, X.-J. Weng, X. Yang, H.-M. Guo, T.-S. Mei, *J. Am. Chem. Soc.* **2019**, *141*, 18970–18976.

[17] F. Romanov-Michailidis, B. D. Ravetz, D. W. Paley, T. Rovis, *J. Am. Chem. Soc.* **2018**, *140*, 5370–5374.

[18] For other examples of reactions catalyzed by moderately electron-deficient $CpIr^{III}$ catalysts, see: a) J. H. Conway, Jr., T. Rovis, *J. Am. Chem. Soc.* **2018**, *140*, 135–138; b) H. Lei, J. H. Conway, Jr., C. C. Cook, T. Rovis, *J. Am. Chem. Soc.* **2019**, *141*, 11864–11869.

[19] E. Tomita, K. Yamada, Y. Shibata, K. Tanaka, M. Kojima, T. Yoshino, S. Matsunaga, *Angew. Chem. Int. Ed.* **2020**, *59*, 10474–10478; *Angew. Chem.* **2020**, *132*, 10560–10564.

[20] For the comparison of the electron-deficiency of the modified $CpRh^{III}$ complexes, see: T. Piou, F. Romanov-Michailidis, M. Romanova-Michaelides, K. E. Jackson, N. Semakul, T. D. Taggart, B. S. Newell, C. D. Rithner, R. S. Paton, T. Rovis, *J. Am. Chem. Soc.* **2017**, *139*, 1296–1310.

[21] a) D. J. Gorin, F. D. Toste, *Nature* **2007**, *446*, 395–403; b) A. Leyva-Pérez, A. Corma, *Angew. Chem. Int. Ed.* **2012**, *51*, 614–635; c) T. M. Figg, S. Park, J. Park, S. Chang, D. G. Musaev, *Organometallics* **2014**, *33*, 4076–4085; d) Y. Park, J. Heo, M.-H. Baik, S. Chang, *J. Am. Chem. Soc.* **2016**, *138*, 14020–14029.

[22] K. M. Engle, T.-S. Mei, M. Wasa, J.-Q. Yu, *Acc. Chem. Res.* **2012**, *45*, 788–802.

[23] a) Z. Chen, B. Wang, J. Zhang, W. Yu, Z. Liu, Y. Zhang, *Org. Chem. Front.* **2015**, *2*, 1107–1295; b) C. Sambiagio, D. Schönbauer, R. Blieck, T. Dan-Huy, G. Pototschnig, P. Schaaf, T. Wiesinger, M. F. Zia, J. Wencel-Delord, T. Besset, B. U. W. Maes, M. Schnürch, *Chem. Soc. Rev.* **2018**, *47*, 6603–6743; c) K. Murali, L. A. Machado, R. L. Carvalho, L. F. Pedrosa, R. Mukherjee, E. N. Da Silva Júnior, D. Maiti, *Chem. Eur. J.* **2021**, *27*, 12453–12508; d) R. Mandal, B. Garai, B. Sundararaju, *ACS Catal.* **2022**, *12*, 3452–3506.

[24] a) A. Tomberg, M. É. Muratore, M. J. Johansson, I. Terstiege, C. Sköld, P.-O. Norrby, *iScience* **2019**, *20*, 373–391; b) G. Liao, T. Zhang, L. Jin, B.-J. Wang, C.-K. Xu, Y. Lan, Y. Zhao, B.-F. Shi, *Angew. Chem. Int. Ed.* **2022**, *61*, e202115221; *Angew. Chem.* **2022**, *134*, e202115221.

[25] Á. Iglesias, R. Álvarez, Á. R. de Lera, K. Muñiz, *Angew. Chem. Int. Ed.* **2012**, *51*, 2225–2228.

[26] G. Li, D. Leow, L. Wan, J.-Q. Yu, *Angew. Chem. Int. Ed.* **2013**, *52*, 1245–1247; *Angew. Chem.* **2013**, *125*, 1283–1285.

[27] E. Tan, O. Quinonero, M. E. de Orbe, A. M. Echavarren, *ACS Catal.* **2018**, *8*, 2166–2172.

[28] For other examples of ether-directed C–H functionalization reactions, see: a) S. Kawamorita, H. Ohmiya, K. Hara, A. Fukuoka, M. Sawamura, *J. Am. Chem. Soc.* **2009**, *131*, 5058–5059; b) J. Oyamada, M. Nishiura, Z. Hou, *Angew. Chem. Int. Ed.* **2011**, *50*, 10720–10723; *Angew. Chem.* **2011**, *123*, 10908–10911; c) J. Oyamada, Z. Hou, *Angew. Chem. Int. Ed.* **2012**, *51*, 12828–12832; *Angew. Chem.* **2012**, *124*, 13000–13004; d) C. W. Liskey, J. F. Hartwig, *J. Am. Chem. Soc.* **2012**, *134*, 12422–12425; e) L, Zhao; X, Shi.; J, Cheng. *ACS Catal.* **2021**, *11*, 2041–2046; f) M. E. Hoque, M. M. M. Hassan, B. Chattopadhyay, *J. Am. Chem. Soc.* **2021**, *143*, 5022–5037; g) L. Zhao, P. Deng, X. Gong, X. Kang, J. Cheng, *ACS Catal.* **2022**, *12*, 7877–7885; h) S. Wang, C. Zhu, L. Ning, D. Li, X. Feng, S. Dong, *Chem. Sci.* **2023**, DOI: 10.1039/D2SC06725K; i) T. Xie, L. Chen, Z. Shen, S. Xu, *Angew. Chem. Int. Ed.* **2023**, e202300199; *Angew. Chem.* **2023**, e202300199.

[29] B. Audic, M. D. Wodrich, N. Cramer, *Chem. Sci.* **2019**, *10*, 781–787.

[30] D. A. Loginov, A. M. Miloserdov, Z. A. Starikova, P. V. Petrovskii, A. R. Kudinov, *Mendeleev Commun.* **2012**, *22*, 192–193.

[31] a) R. P. Hughes, D. C. Lindner, L. M. Liable-Sands, A. L. Rheingold, *Organometallics* **2001**, *20*, 363–366; b) J. Yuan, R. P. Hughes, A. L. Rheingold, *Inorg. Chim. Acta* **2010**, *364*, 96–101.

[32] Deposition Number CCDC 2123310 for **9** contains the supplementary crystallographic data for this paper. These data can be obtained free of charge from The Cambridge Crystallographic Data Centre via www.ccdc.cam.ac.uk/data_request/cif.

[33] For selected examples of C–H amidation reactions using sulfonyl azides as a reactant, see: a) J. Y. Kim, S. H. Park, J. Ryu, S. H. Cho, S. H. Kim, S. Chang, *J. Am. Chem. Soc.* **2012**, *134*, 9110–9113; b) J. Kim, J. Kim, S. Chang, *Chem. Eur. J.* **2013**, *19*, 7328–7333; c) M. R. Yadav, R. K. Rit, A. K. Sahoo, *Org. Lett.* **2013**, *15*, 1638–1641; d) Q.-Z. Zheng, Y.-F. Liang, C. Qin, N. Jiao, *Chem. Commun.* **2013**, *49*, 5654–5656; e) V. S. Thirunavukkarasu, K. Raghuvanshi, L. Ackermann, *Org. Lett.* **2013**, *15*, 3286–3289; f) D. Lee, Y. Kim, S. Chang, *J. Org. Chem.* **2013**, *78*, 11102–11109; g) J. Kim, S. Chang, *Angew. Chem. Int. Ed.* **2014**, *53*, 2203–2207; *Angew. Chem.* **2014**, *126*, 2235–2239; h) T. Kang, Y. Kim, D. Lee, Z. Wang, S. Chang, *J. Am. Chem. Soc.* **2014**, *136*, 4141–4144.

[34] B. Sun, T. Yoshino, S. Matsunaga, M. Kanai, *Adv. Synth. Catal.* **2014**, *356*, 1491–1495.

[35] a) U. Mayer, V. Gutmann, W. Gerger, *Monatsh. Chem.* **1975**, *106*, 1235–1257; b) M. A. Beckett, G. C. Strickland, J. R. Holland, K. S. Varma, *Polymer* **1996**, *37*, 4629–4631; c) G. C. Welch, L. Cabrera, P. A. Chase, E. Hollink, J. D. Masuda, P. Wei, D. W. Stephan, *Dalton Trans.* **2007**, 3407–3414.

[36] E. M. Simmons, J. F. Hartwig, *Angew. Chem. Int. Ed.* **2012**, *51*, 3066–3072.

[37] To shed light on the Ir(V)-nitrenoid formation process, Hammett plot analysis was conducted for a series of *para*-substituted sulfonyl azides (Figure S13). As the result, a relatively small negative ρ (–0.11) was observed, which implied that electron-donating groups on sulfonyl azides accelerated this reaction, but the influence was moderate compared to the related C–H amidation reaction in which a primary KIE was not observed. See: Y.-F. Zhang, B. Wu, Z.-J. Shi, *Chem. Eur. J.* **2016**, *22*, 17808–17812.

[38] a) D. Lapointe, K. Fagnou, *Chem. Lett.* **2010**, *39*, 1118–1126; b) L. Ackermann, *Chem. Rev.* **2011**, *111*, 1315–1345; c) D. L. Davies, S. A. Macgregor, C. L. McMullin, *Chem. Rev.* **2017**, *117*, 8649–8709.

[39] Our preliminary calculation suggested that the **Ir-X** might be better described as an Ir(III)-nitrene or an Ir(IV)-nitrene radical rather than Ir(V)-nitrenoid due to the ligand field inversion, and the Cp^EIr complex tends to adopt a lower oxidation state than the Cp*Ir complex (for details, see the Supporting Information). For the ligand field inversion, see: a) R. Hoffmann, S. Alvarez, C. Mealli, A. Falceto, T. J. Cahill, III, T. Zeng, G. Manca, *Chem. Rev.* **2016**, *116*, 8173–8192. (b) K. M. Carsch, I. M. DiMucci, D. A. Iovan, A. Li, S.-L. Zheng, C. J. Titus, S. J. Lee, K. D. Irwin, D. Nordlund, K. M. Lancaster, T. A. Betley, *Science* **2019**, *365*, 1138–1143.

[40] Additional calculation results were shown in the Supporting Information.

[41] J.-B. Liu, X.-H. Sheng, C.-Z. Sun, F. Huang, D.-Z. Chen, *ACS Catal.* **2016**, *6*, 2452–2461.

Entry for the Table of Contents

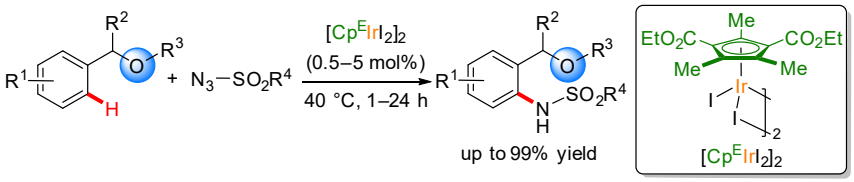

A highly electron-deficient cyclopentadienyl iridium(III) complex was developed ($[Cp^EIrI_2]_2$). This complex effectively catalyzed weakly coordinating ether-directed C–H amidation reactions under mild reaction conditions. Mechanistic experiments and DFT calculations indicated that the high catalytic activity of the $[Cp^EIrI_2]_2$ complex is attributed to its highly electron-deficient nature.

Institute and/or researcher Twitter usernames: @tokyotech_en @KenTanaka_Lab @HokkaidoUni @MatsunagaGroup